Chapter-6

Synthesis and Characterization of Ti-Mo-Fe alloy- S53P4 Bioactive glass composite

6.1 Introduction

In this chapter, we have synthesis the Ti alloy by alloying Molybdenum and iron metals. This is used as a matrix to make composite of above alloy with bioactive glass. Referring to phase discussion and crystal structure of ti alloys, in second chapter, Mo metal comes under the category of beta stabilizer which favors the formation of stable beta phase. It has the crystal structure of body centred cubic and it's atomic number is 42. It doesn't found in free state iin the nature. Molybdenum-bearing enzymes are by far the most common bacterial catalysts for breaking the chemical bond in atmospheric molecular nitrogen in the process of biological nitrogen fixation. At least 50 molybdenum enzymes are now known in bacteria, plants, and animals, although only bacterial and cyanobacterial enzymes are involved in nitrogen fixation[1].

Molybdenum contributes corrosion resistance to type-300 stainless steels (specifically type-316) and especially so in the so-called super austenitic stainless steels (such as alloy AL-6XN, 254SMO and 1925hMo). Molybdenum increases lattice strain, thus increasing the energy required to dissolve iron atoms from the surface. Because of its lower density and more stable price, molybdenum is sometimes used in place of tungsten[2]..

The solubility limits of alloying elements, Mo, Nb and Ta in Ti are 8, 22 and 52 wt.%, respectively. Thus, Mo is an effective β stabilizer. Moreover, Mo is less toxic than Al and V.

Ti–Mo alloy will be the good choice for the implant materials in tissue and damaged organs because of its good biological compatibility. The phase diagram of Ti-Mo alloy reveals these facts. Therefore we can control phase stability, which leads to desirable mechanical and physical properties through an optimal choice of alloy composition and heat treatment route [3].

It is well known that solution heat-treating β Ti alloys at high temperatures and then cooling them rapidly may lead to microstructures composed of martensite and β phase. The two metastable phases, i.e., orthorhombic martensite (α″) and the bcc phase, display low elastic modulus values and mechanical strength[4].

Iron (Fe) is a low-cost material which also reduces α to β transformation temperature of titanium and is also considered as a β stabilizer element. It also positively affects the remodeling of the bone, osteogenesis and other functional mechanisms in the body. So it could be used as an alloying element in a smaller amount for biomedical applications. [5,6].

Current work comprises the synthesis of Ti-8Mo-2Fe alloy matrix by powder metallurgical route which is reinforced with S53P4 bioactive glass in the percentage range of 0 - 20%.. The main aim of current work is to observe and optimize the mechanical and biological properties of both alloy and S53p4 bioactive glass to match the resultant biomechanical properties with the cortical bone and to remove the drawback of coated alloys by incorporating the glass into the matrix instead of coating.

6.2 Alloy Preparation

Titanium (Ti) metal powder is mechanical alloyed (MA) with eight weight percent of Mo and two weight percent of Iron (Fe) metal powders in a high energy ball mill containing stainless steel vial along with steel balls for the synthesis of titanium alloy powder at room temperature. The powder-to-ball weight ratio was maintained at 15:1. The vial was loaded with mixture of all three powder in above mentioned ratio in an controlled argon-filled glove-box to prevent oxidation of metals.

The mill was operated to 25 h for powder alloy preparation with alternative intervals of 10 minutes to prevent of temperature raise. Because of the ductility of metal powders; the milling is carefully controlled by adding a small amount of process control agent, (PCA), i.e., two weight % ethanol to the milling process was added. The PCA increases the milling efficiency by refreshing metal surface contacts. It also reduces the welding of the powder particles to each other and prevents the oxidation and contamination of material. [32].

6.3 Glass Preparation

The glass batch containing following composition 56.6 % B_2O_3,18.5 % CaO, 5.5%Na_2O, 11.1% K_2O,4.6 %MgO,3.7% P_2O_5, as weight percentage were prepared taking the starting material as Quartz(99% SiO_2), Magnesium Oxide (99%MgO) Calcium Carbonate (99%$CaCO_3$), Sodium Carbonate (99%Na_2CO_3), Potassium carbonate (98%K_2CO_3) and Boric acid (99%B_2O_3) . The materials were mixed for 30 minutes in a mortar pestle. These reagents were then melted in a platinum crucible for 4.5 h in an electric furnace at 1300^0C. Further, the glass melt was water quenched. Resultant glass was crushed and ball milled in the pot mill to bring in the powder form.

6.4 Composite preparation

The mechanically alloyed metal powder matrix was reinforced with 5, 10 and 20 percentage of melt-quenched S53P4 bioactive glass (Table 1) and ball milled for 20 minutes for homogeneous mixing, and 0.3 % of carboxyl methyl cellulose (CMC) is added as an organic binder. A uniaxial cold press machine is used to consolidate the composites under the pressure of 550 MPa in the form of bars and pallets. The green compacts were pre-sintered first at 700^0C for 1 h for removal of the binder afterward sintered in a vacuum tube furnace with the holding time of 5 h at 1150 °C with the heating rate of 8 °C/min. The cooling is achieved first at 5 °C/min till 900°C and then allowed to cool at a faster rate of 40°C/min.

6.5 Result and Discussion

6.5.1 Scanning Electron Microscopy (SEM)

The SEM micrographs of composites are shown in Fig 6.1 . Fig (a) shows the micrograph of pure alloy phase, where, the structure is of trapping nature with some sort of brittle intermetallic compound trapping between them. The smaller amount of glass phase which seems to try to encapsulates the alloy (M2) is also visible in microstructures (c) where the reinforcement of BAG is small (5%). Figure 6.1 (d) reveal that the alloy particles are settled into alloy structure more and that is why appears to be in glassy phase as the percentage of bioactive glass changes from 10% (M3) to 20 % (M4). The increment in the embedded nature of metal particles in glassy phase signify the uniform sprayed of melted glass on the surface of the composite. The increase in non-homogenous pores with the reinforced percentage of bioactive glass are also clearly visible in micrographs.

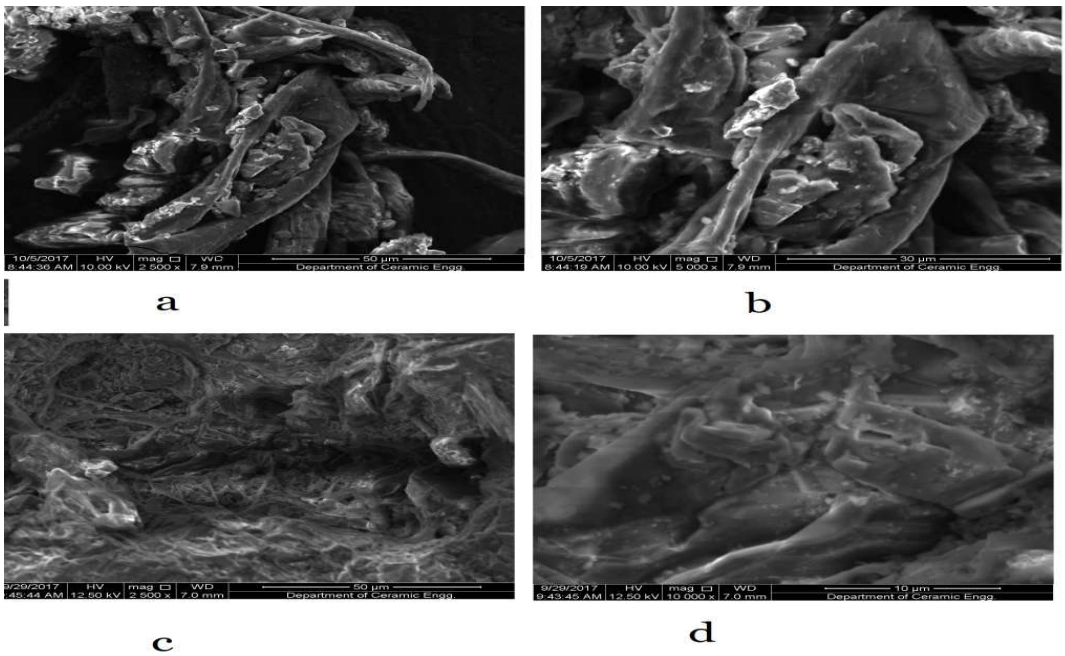

Fig.6.1 SEM micrographs of (a) pure alloy M1 (b)Alloy + 5%BAG M2 (c) Alloy +10%BAG M3 (d)Alloy + 20%BAG M4

6.5.2 Physio-mechanical Properties

Fig 6.1 (a) and 6.2 (b) depicts the apparent porosity and bulk density of the samples respectively with more pouncing way than previous while bulk density decreases. The maximum porosity i.e. 28 % is obtained from the reinforcement of sample containing 20 % of bioactive glass. This is due to the increase in bioactive glass content. A little proportion of the reinforcing phase may occupy the internal voids of alloy matrix easily, so the densification affects by smaller amounts but as the percentage of reinforcement increases, the internal friction and resulting bridging effect during single-action pressing effectively suppresses the densification. This leads to lower density of the composites.

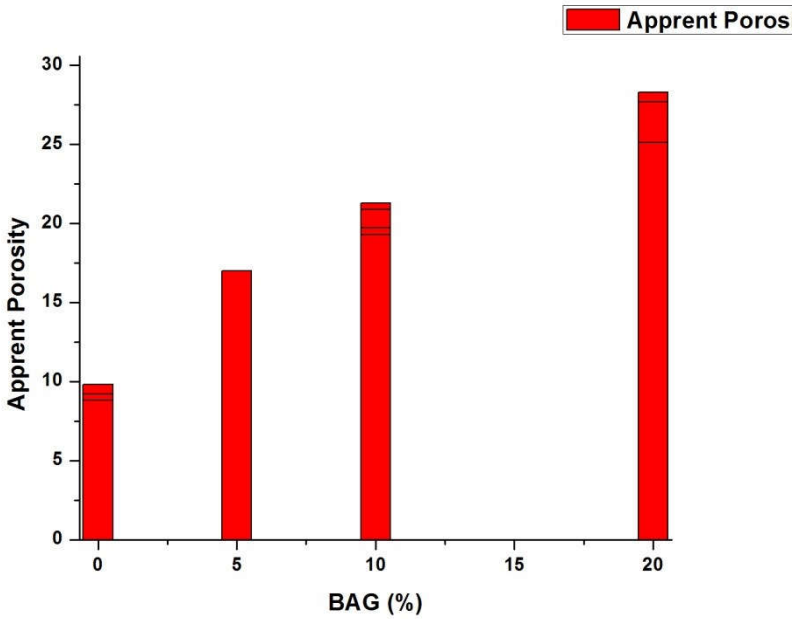

Fig.6.2 (a) Apparent porosity of all the samples (M1, M2, M3, M4)

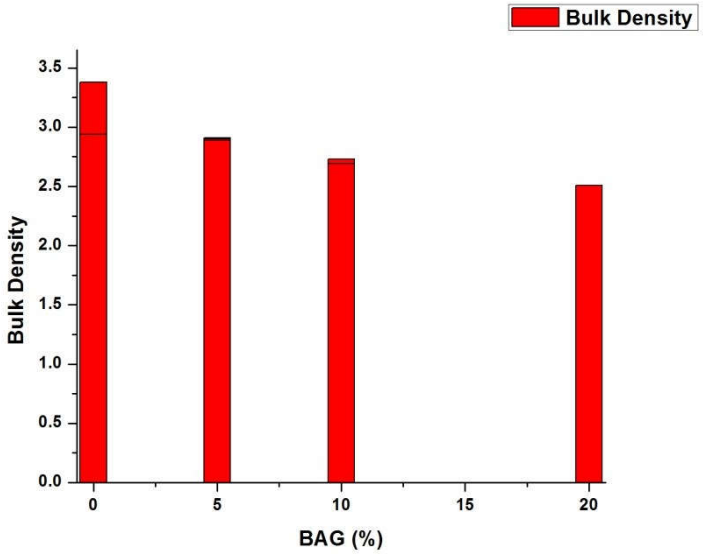

Fig.6.2 (b) Bulk Density of all the samples (M1, M2, M3, M4)

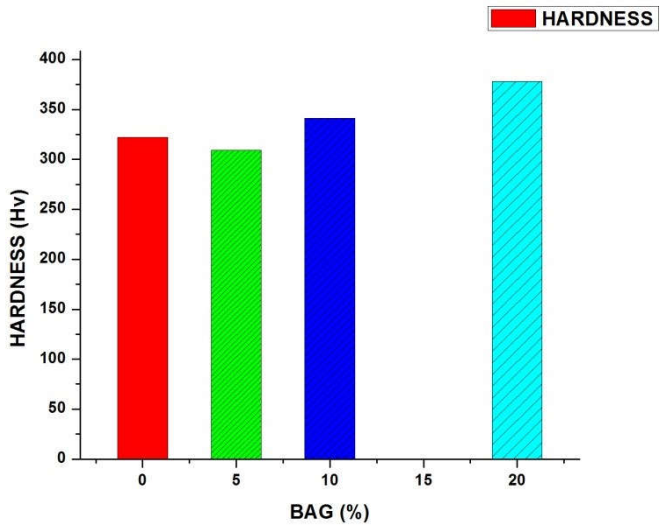

Fig.6.3.Vickers's Hardness of all the samples (M1, M2, M3, M4)

The results of Vickers's hardness measurement of the reinforced alloy are shown in figure 6.4. The hardness of pure alloy matrix (M1) increases (325 Hv) as compared to commercial pure Ti and Ti6Al4V alloy .Further, the graph also indicates that hardness decreases with the reinforced percentage of bioactive glass, reaching to the value of 368 Hv at 20% of reinforcement but it is still superior to the hardness of the cortical bone [40]. Although the amount of intermetallic increases in composites ,which would have raised the hardness of the composites .

The measured elastic modulus of prepared composites is represented in fig.6.5. It shows that the pure alloy matrix (M1) possesses the elastic modulus of 93 GPa which is lower than the commercially available Ti-6Al-4V alloy (110 GPa) [41]. Figure also shows the modulus value decreases on increasing the reinforcement of silicate bioactive glass. The value reaches up to 66 GPa at 20 % reinforcement which is an essential requirement of the implant to minimize the stress shielding effect [7].

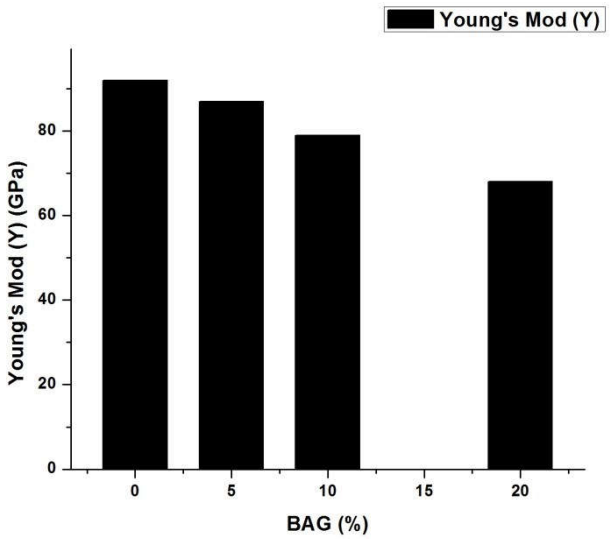

Fig.6.4 Elastic Modulus of all the samples (M1, M2, M3, M4)

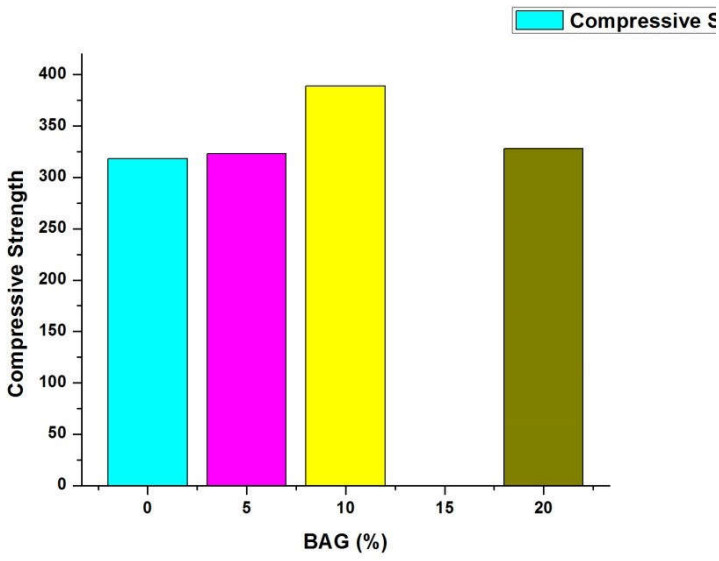

Fig. 6.5 Compressive Strength of all the samples (M1, M2, M3, and M4)

6.5.3 In vitro Bioactivity

To analyze the formation of hydroxyl carbonated apatite (HCA) layer on immersing the samples in SBF solution, the pH behavior of SBF solution has been noted down during different immersion time. Figure 6.7 shows the change of pH in different immersion time up to 5 days. It is clear from the graph that the pH value of composite samples , M3, M4, increases to 8.30, 8.6 respectively within five days as compared to the initial pH (7.4) of SBF solution at 37^0C under physiologic conditions.

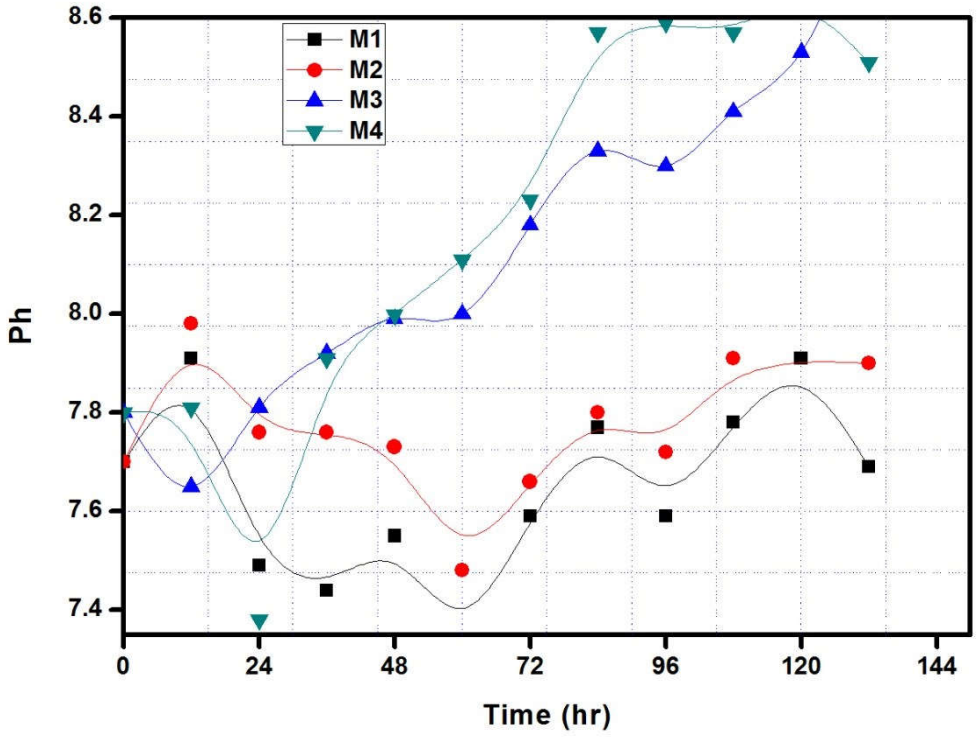

Fig. 6.6 Variation of pH for all samples with respect to the immersing time

The increase in pH in composites, M3 and M4 illustrate the dissolution of cations and the network modifiers (such as Na+ and K+) from the surface of the glass.[44] The different value of pH after 5 day for the M1, M2 and M3 composites are due to the difference in weight percentage of bioactive glass in the composition. These cations from the glass along with the phosphate ions released from the SBF solution give rise to the formation of the hydroxyl appetite layer [9.10].

The graph also depicts that the rate of change of pH also increases with the reinforcing percentage of bioactive glass. The growth of hydroxyl carbonated apatite layer is formed on the surface of samples grown better in the form of agglomerates.

6.5.3 X-Ray diffraction analysis of composites

X-ray diffraction patterns were observed by XRD machine .Phase identification analysis was carried out by comparing the XRD patterns of the composites to the standard database of PCPDFWIN represented in Figure and it shows the XRD of the composite samples before dipping them into the simulated body fluid (SBF). Before being soaked in SBF solutions, XRD absorption peak was not showing for the bioactive samples, except for one upper dick like peak range from 20° to 30°, which is due to silica network. So it is clear that surface of bioactive composite samples were amorphous in nature before being soaked in simulated body fluid (SBF) solution. While Figure b indicates the XRD plots of the composites having bioactive glass soaked in the simulated body fluid (SBF) solution for 14 days. After being soaked in the SBF solution for 14 days, one diffraction peak was observed at 31.9°, which showd the presence of the HA phase. These peaks were identified by standard JCPDS cards numbered 89-6495

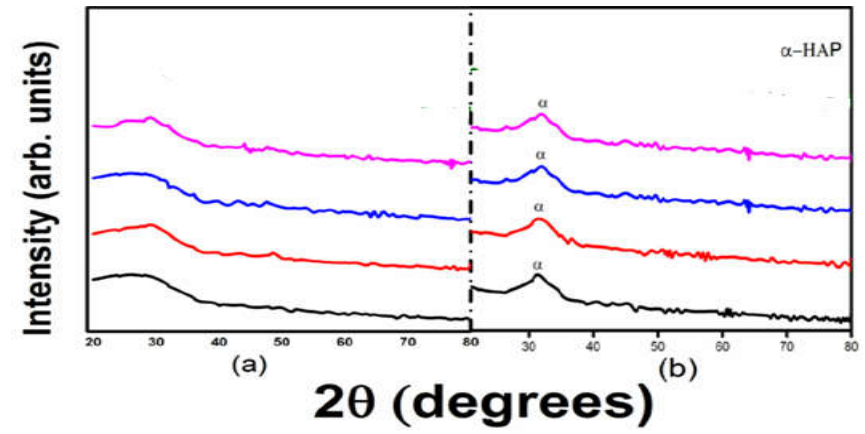

Fig 6.7 XRD of composites before and after soaking in SBF

6.5.4 Cell culture

Human osteosarcoma cells U2-OS were procured from American Type Culture Collection (ATCC), Manassas, USA and was maintained in RPMI 1640 (Invitrogen, Carlsbad, CA), supplemented with 10% fetal bovine serum (Hyclone, Logan, UT), 100 U/ml penicillin and 100 µg/ml streptomycin (Invitrogen, Carlsbad, CA), henceforth considered as complete medium.

Treatment of U2-OS cells with the increasing concentration of the compound S1, S2, S3, and S4 shows a dose-dependent augmentation of the cytotoxicity in the tumor cells (Fig.9 A-D). Among the products, M1 and M3 are more tolerant compared to the other two formulations. Comparative analysis of the cytotoxicity at concentrations of 25 and 100 µg, suggests that the compounds at a higher level are severely toxic to the cells and only relatively safe at the lower concentration tested.

For the comparison between the groups, unpaired student's t-test or one way ANOVA followed by Tukey's post hoc test have been used. The data represented as mean ± SD

(standard deviation) and the test was conducted three times for each sample. The significant differences were considered for 'p' value < 0.05. p< 0.001 (****).

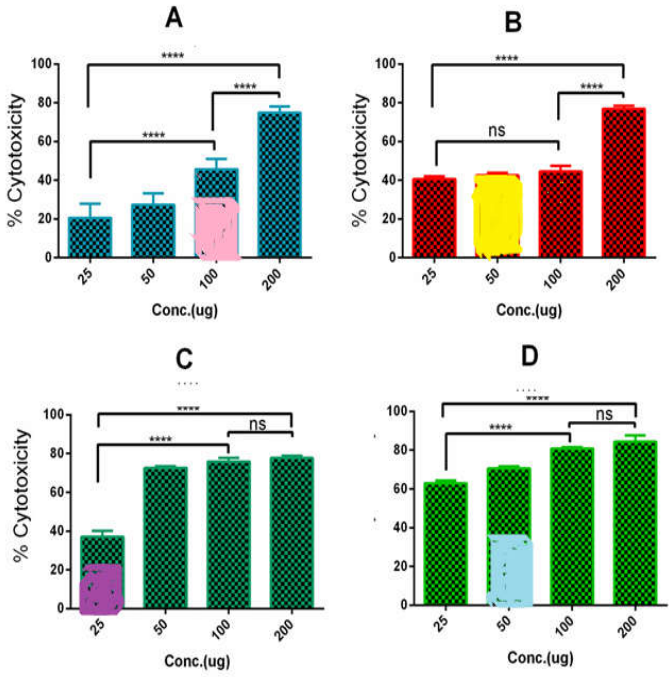

Fig.6.8. The concentration-dependent killing of the U2-OS cells in the presence of M1, M2, M3, and M4.

We tested the proliferation of the cells in the presence of varying concentration of the above compounds. Our data suggested that compound M1 and M3 supports the growth of the tumor cells at a concentration of 25 µg (Figure 10). However, both M2 and M4 are not tolerant to the tumor cells and hinder the proliferation of the cells. Increasing the concentration of the compound largely detrimental for the tumor cells growth for all the compounds tested (Figure 10).

From the above results, it is clear that compounds are relatively safe at low concentration; however, at higher concentration the formulations may be detrimental for the cells.

This also suggests that the compound may be used for the implant since osteocytes like U2-OS are present in association with bone tissues where the possible implantation could be made. This indicates that the compound may be biologically compatible for real-life scenario.

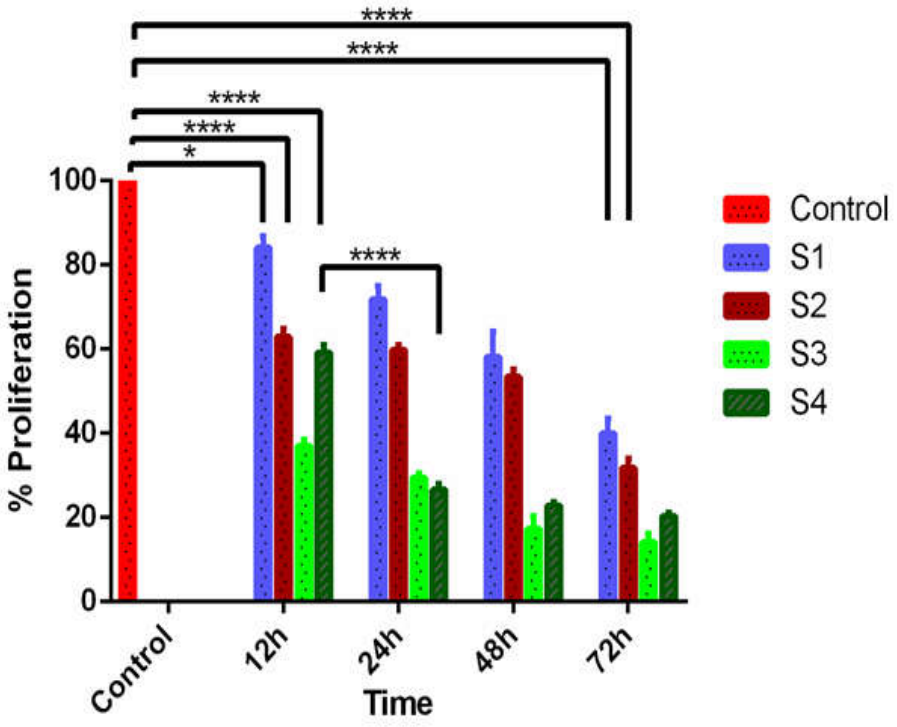

Fig 6.9. Time dependent proliferation of the U2-OS cells in the presence of varying concentrations of M1, M2, M3, and M4.

4.6 Corrosion Study

The corrosion study has been carried out from weight loss method to study the effect of SBF on the prepared samples. Fig 12 depicts the relation between the corrosion rate of tested samples and immersion time. This graph shows that the composites S2, S3, and S4

comprise 1393 B3 BAG initially have a high corrosion rate as compared to pure alloy S1. This is probably because of the fast degradation rate of borate bioactive glass which leads to the weight loss of the samples [11,12,13]. Due to this fact, initially the corrosion rate becomes high, but as the time passes, the rate of weight loss decreases and hence the corrosion rate decreases and approaches nearly to .0015 millimetre per year (mmpy).

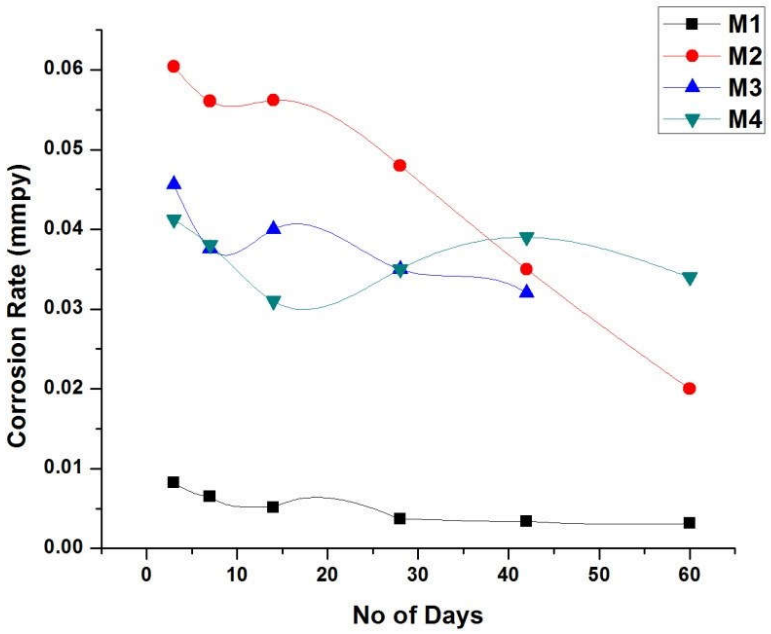

Fig.6.10 corrosion rate of pure alloy (M1) and all composites containing BAG (M2, M3, M4)

The above findings of our composites indicating that Composite M3 composite which is containing 10 % S53P4 bioactive glass in Ti-8Mo-2Fe alloy matrix seems to be well optimized composition because of considerably greater mechanical properties i.e. superior compressive strength, low Young's modules, optimum density and hardness as compared to pre-existing Ti implants and more closely matched mechanical and biological properties with that of cortical bone.

References

1.Xin-Yuan Huang, Da-Wei Hu, Fang-Jie Zhao, Molybdenum: *Mo*re than an essential element, *Journal of Experimental Botany*, 2021;

2.Liu, Y.; Xie, Y.; Cui, S.; Yi, Y.; Xing, X.; Wang, X.; Li, W. Effect of Mo Element on the Mechanical Properties and Tribological Responses of CoCrFeNiMo*x* High-Entropy Alloys. *Metals* **2021**,

3.John Emsley, *Nature's Building Blocks: An A-Z Guide to the Elements*, Oxford University Press, New York, 2nd Edition, 2011.

4.Hsueh-Chuan Hsu a,b, Shih-Ching Wu a,b, Shih-Kuang Hsu a,b, Tien-Yu Chang c, Wen-Fu Ho Effect of ball milling on properties of porous Ti–7.5Mo alloy for biomedical applications. Journal of Alloys and Compounds 582 (2014) 793–801.

5. Abbaspour N, Hurrell R, Kelishadi R. Review on iron and its importance for human health. *J Res Med Sci*. 2014;19(2):164-174.

6. The Effect of Fe Addition on the Mechanical Properties of Ti–6Al–4V Alloys Produced by the Prealloyed Powder Method*1 Osamu Kanou, Nobuo Fukada and Masashi Hayakawa Materials Transactions, Vol. 57, No. 5 (2016) pp. 681 to 685.

7. Ho WF, A comparison of tensile properties and corrosion behavior of cast Ti – 7.5Mo with c. p. Ti, Ti – 15Mo and Ti – 6Al – 4V alloys. J of Alloys and compounds 2008; 464: 580–583.

8. M. Dekker, Manganese and its role in biological process –METAL IONS IN BIOLOGICAL SYSTEMS edited by Astrid Sigel and Helmut Sigel. 2000; 7:3.

9. SilviaSprianoa, SeijiYamaguchi et al. A critical review of multifunctional titanium surfaces: New frontiers for improving osseointegration and host response, avoiding bacteria contamination. Acta Biomaterialia 2018; 79:1-22

10.Tripathi H, Rath C, et al. Structural, physico-mechanical and in-vitro bioactivity studies on SiO2–CaO–P2O5–SrO–Al2O3 bioactive glasses. Materials Science & Engineering C. 2019; 94: 279–290.

11 Tripathi H, Kumar S, et al. Structural characterization and in vitro bioactivity assessment of SiO 2 – CaO – P 2 O 5 – K 2 O – Al 2 O 3 glass as bioactive ceramic material. Ceramics International 2015 41: 11756–11769.

12. Rahaman MN, Bioactive ceramics and glasses for tissue engineering, in: Aldo R Boccaccini, P.X. Ma. Tissue Engineering Using Ceramics and Polymers wood head publishing 2014.

13. Su Y, Ouyang Q, et al. Composite structure modeling and mechanical behavior of particle reinforced metal matrix composites. Materials Science & Engineering A. 597 (2014) 359–369.